View metadata, citation and similar papers at core.ac.uk

brought to you by CORE

provided by Infoscience - École polytechnique fédérale de Lausanne

SIAM J. NUMER. ANAL.
Vol. 43, No. 5, pp. 1912–1933

© 2005 Society for Industrial and Applied Mathematics

SPECTRAL METHODS BASED ON PROLATE SPHEROIDAL WAVE FUNCTIONS FOR HYPERBOLIC PDEs*

Q.-Y. CHEN†, D. GOTTLIEB†, AND J. S. HESTHAVEN†

Abstract. We examine the merits of using prolate spheroidal wave functions (PSWFs) as basis functions when solving hyperbolic PDEs using pseudospectral methods.

The relevant approximation theory is reviewed and some new approximation results in Sobolev spaces are established. An optimal choice of the band-limit parameter for PSWFs is derived for single-mode functions.

Our conclusion is that one might gain from using the PSWFs over the traditional Chebyshev or Legendre methods in terms of accuracy and efficiency for marginally resolved broadband solutions.

Key words. prolate spheroidal wave functions, spectral methods, penalty methods

AMS subject classifications. 65M70, 41A30, 65D05

DOI. 10.1137/S0036142903432425

1. Introduction.

Pseudospectral methods for PDEs [6, 13] approximate the solution by classical polynomials (usually Chebyshev or Legendre) or trigonometric polynomials. The main reason for their success is the spectral accuracy, i.e., the convergence rate depends only on the smoothness of the functions being approximated. This comes at a price, however, as the norm of the differentiation matrix is proportional to the square of the number, N, of interpolation points (or the order of the polynomials), resulting in small time-steps ($\sim N^{-2}$) [14], when using an explicit schemes for time integration.

This stringent restriction on the time-step can be attributed to the basis functions being classical orthogonal polynomials, the roots of which cluster near the boundaries of the interval, e.g., the smallest distance between any two roots of a Chebyshev polynomial of degree N is $O(N^{-2})$. In [18], it was suggested to use a singular mapping to change the basis functions to overcome this restriction, and this technique has been successfully used by many people (e.g., [1, 2, 10, 16, 20, 21]). However, as shown in [16, 20] this mapping only allows for doubling the time-step for practical N. If N is large, however, the time-step can be increased to scale as $O(N^{-1})$ [18, 10] without sacrificing the accuracy as the impact of the singular mapping becomes dominated by the finite precision. The mapping destroys the quadrature properties of the roots of the classical polynomials, which may be a disadvantage in certain applications, e.g., when filtering is needed or if integrals must be computed as part of the solution, e.g., in spectral element methods.

In this paper we assess the performance of pseudospectral methods based on prolate spheroidal wave functions (PSWF – ψ_k^c) rather than on polynomials. In [25], the authors demonstrate the merits of using PSWFs for the interpolation, integration

*Received by the editors July 25, 2003; accepted for publication (in revised form) April 13, 2005; published electronically December 8, 2005.

http://www.siam.org/journals/sinum/43-5/43242.html

†Division of Applied Mathematics, Brown University, Box F, Providence, RI 02912 (cqy@cfm.brown.edu, dig@cfm.brown.edu, Jan.Hesthaven@brown.edu). The work of the second author was partly supported by the NSF under contract DMS-0207451 and by HyperComp under contract HPC/F33615-01-c-1866. The work of the third author was partly supported by the NSF under contract DMS-0074257 and through NSF Career Award DMS-0132967, by ARO under contract DAAD19-01-1-0631, and by the Alfred P. Sloan Foundation through a Sloan Research Fellowship.

Downloaded 11/26/12 to 128.148.252.35. Redistribution subject to SIAM license or copyright; see http://www.siam.org/journals/ojsa.php

Downloaded 11/26/12 to 128.148.252.35. Redistribution subject to SIAM license or copyright; see http://www.siam.org/journals/ojsa.php

(quadrature), and differentiation of band-limited functions. They show, among other things, that for a prescribed accuracy fewer grid points are required for interpolation and integration than with Chebyshev polynomials. Furthermore, the differentiation matrix has a smaller condition number, approaching $O(N^{3/2})$, which suggest the possibility of increasing the time-step significantly for large values of N.

These basic observations have led to a surge of recent activity in the development of methods based on PSWFs, although the topic itself remains in its infancy. In [4, 5], the author studied the feasibility of using PSWFs as the basis functions in spectral element methods. More recently, in [3] Beylkin and Sandberg developed a two-dimensional solver for the acoustic wave equation by using a basis of approximate PSWFs. However, even basic aspects of approximation and stability theory for methods based on PSWFs remain unknown.

In this work we consider some of these issues, in particular in the context of solving hyperbolic PDEs by constructing pseudospectral methods based on quadrature points and roots associated with the PSWFs. The first step in this direction is to review and expand the relevant approximation theory. We discuss basic approximation properties such as the number of points per wavelength required to recover a meaningful result and show that only two points per wavelength are needed. Thus, the PSWF expansion recovers the Nyquist limit from Fourier theory, although defined on a finite interval. This should be contrasted with polynomial expansions where asymptotic estimates show that at least π points per wavelength are needed [14]. We derive a new result that demonstrates the spectral accuracy of approximations of smooth functions by the PSWFs.

Several variants of pseudospectral PSWF methods based on different interpolation points are subsequently discussed, the main differences being in the definition of the interpolation points, e.g., we consider genuine Gauss-type quadrature points as well as Gauss–Lobatto like points defined as the roots of $(1-x^2)(\psi_N^{2c})'$, where ψ_N^{2c} is the Nth order PSWF with bandwidth $2c$—this approach is clearly inspired by results from classical polynomials although they are in this case not associated with a quadrature. The performance of these slightly different methods are essentially equivalent although the latter choice is more appropriate for solving initial-boundary value problems. We finally consider the performance of these methods for solving a scalar hyperbolic equation as well as hyperbolic systems.

The results of our study can be summarized as follows.

- A practical relation between the two parameters, c and N, is $N = c$ to allow convergence.
- With this choice one observes spectral accuracy. When the solution is broadband and marginally resolved, the PSWF-based method is more accurate than the Chebyshev method with the same number of terms, i.e., generally more efficient.
- Theoretically the time-step Δt can be taken as $O(N^{-\frac{3}{2}})$ if $N \simeq \frac{2}{\pi}c$. However, the accuracy deteriorates significantly in this case.

The remaining part of the paper is organized as follows. In section 2, we present some mathematical background and define the PSWFs. Section 3 contains some approximation results, while section 4 deals with the construction of pseudospectral methods based on PSWFs. We discuss their stability and solve scalar hyperbolic equations as well as hyperbolic systems. In the appendix, we give the details of the proof of the main approximation result.

Downloaded 11/26/12 to 128.148.252.35. Redistribution subject to SIAM license or copyright; see http://www.siam.org/journals/ojsa.php

2. Preliminaries. In this section, we shall summarize the notation and some general results regarding the PSWFs.

2.1. Prolate spheroidal wave functions. A function $f(x) : [-1, 1] \to [-1, 1]$ is band-limited if there exist a $c > 0$ and a function $\phi(t) \in L^2[-1, 1]$ such that

$$f(x) = F_c(\phi)(x) = \int_{-1}^{1} e^{icxt}\, \phi(t)\, dt.$$

It is easy to see that F_c: $L^2[-1, 1] \to L^2[-1, 1]$ is a compact operator, i.e., that it has eigenvalues $\lambda_0, \lambda_1, \lambda_2, \ldots$, with the property $|\lambda_{i-1}| \geq |\lambda_i|\ \forall i > 0$. We shall denote by $\psi_j^c(x)$ the eigenfunction corresponding to λ_j. Then

$$\lambda_j\ \psi_j^c(x)\ =\ \int_{-1}^{1} e^{icxt}\ \psi_j^c(t)\ dt, \qquad x \in [-1, 1], \tag{2.1}$$

and the eigenfunctions, $\{\psi_j^c\}_{j=0}^{+\infty}$, are the PSWFs. We choose to normalize them so that $\|\psi_j^c\|_{L^2[-1,1]} = 1$.

One easily checks that the PSWFs also satisfy

$$\mu_j\ \psi_j^c(x)\ =\ \int_{-1}^{1} \frac{\sin(c(x-t))}{x-t}\ \psi_j^c(t)\ dt, \qquad x \in [-1, 1],$$

where

$$\mu_j = \frac{c}{2\pi}|\lambda_j|^2.$$

The following theorem gives some properties of the PSWFs (see [22, 25] and the references therein).

THEOREM 2.1. *For all $c \geq 0$,*

- *ψ_0^c, $\psi_1^c, \ldots$ are real, orthonormal, smooth, and complete in $L^2[-1, 1]$, and they form a Chebyshev system* [17] *on $[-1, 1]$;*
- *the ψ_k^c with even k are even functions, and those with odd k are odd;*
- *$\lambda_j = i^j|\lambda_j| \neq 0$, where i is the complex unit;*
- *among $\{\mu_j\}_{j=0}^{\infty}$, about $2c/\pi$ are very close to 1; order $\log(c)$ decay exponentially from 1 to nearly 0; the remaining ones are very close to 0.*

Furthermore, there exists a strictly increasing positive sequence $\chi_0, \chi_1, \ldots$, such that

$$\Big((1 - x^2)(\psi_j^c(x))'\Big)' + \big(\chi_j - c^2x^2\big)\psi_j^c(x) = 0. \tag{2.2}$$

When $c = 0$, the above equation reduces to the classic singular Sturm–Liouville problem with $p(x) = 1 - x^2$, $q(x) = 0$, $\omega(x) = 1$, and $\chi_j = j(j + 1)$, i.e., the PSWFs with $c = 0$ are the normalized Legendre polynomials [6, 13].

Following [25], one can evaluate ψ_j^c by expressing it as

$$\psi_j^c(x) = \sum_{k=0}^{\infty} \beta_k^j \overline{P}_k(x), \qquad j = 0, 1, 2, \ldots, \tag{2.3}$$

where $\overline{P}_k$ is the normalized Legendre polynomial of degree k. Substituting (2.3) into (2.2) and using the properties of the Legendre polynomials one obtains an eigenvalue problem

$$(A - \chi_j \cdot I)\beta^j = 0. \tag{2.4}$$

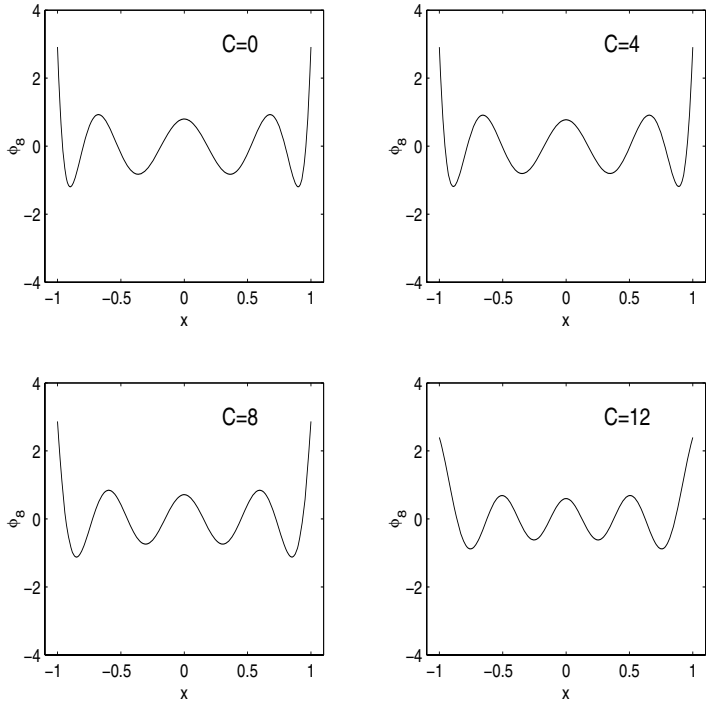

FIG. 2.1. $\psi_8^c(x)$ *for different values of* c.

Here A has the form [25]

$$\begin{cases} A_{k,k} = k(k+1) + \dfrac{2k(k+1)-1}{(2k+3)(2k-1)}\, c^2, \\ A_{k,k+2} = \dfrac{(k+2)(k+1)}{(2k+3)\sqrt{(2k+1)(2k+5)}}\, c^2, \\ A_{k+2,k} = A_{k,k+2} \end{cases}$$

for $k = 0, 1, 2, \ldots$, where the remaining entries of A are zeros.

Since ψ_j^c is smooth, the coefficients β_k^j decay superalgebraically with respect to k. The following theorem [25] offers guidelines on where to truncate (2.3) to ensure a certain accuracy in the approximation of ψ_j^c.

THEOREM 2.2. *Assume* ψ_m^c *is the* m*th PSWF with band-limit* c*, and* λ_m *is the corresponding eigenvalue. If*

$$k \geq 2(\lfloor e \cdot c \rfloor + 1), \tag{2.5}$$

then $\forall c > 0$,

$$\left| \int_{-1}^{1} \psi_m^c(x) \overline{P_k(x)}\, dx \right| < \frac{1}{\lambda_m} \left(\frac{1}{2}\right)^{k-1}. \qquad \square$$

Solving (2.4) and using the corresponding eigenvector in the truncated version of (2.3) allows for the computation of one PSWF (Figure 2.1) for different values of the

Downloaded 11/26/12 to 128.148.252.35. Redistribution subject to SIAM license or copyright; see http://www.siam.org/journals/ojsa.php

Downloaded 11/26/12 to 128.148.252.35. Redistribution subject to SIAM license or copyright; see http://www.siam.org/journals/ojsa.php

band-limit, c. In Figure 2.1, we note that the zeros of the PSWF move toward the center as c increases, approaching a uniform distribution. This observation suggests that by choosing a suitable $c > 0$ the PSWF method needs fewer points per wavelength to accurately resolve a wave problem as compared to approximations based on classical orthogonal polynomials. However, it also suggests that if one chooses c too large for a fixed N, the PSWF is unable to represent functions defined on the whole interval.

3. Approximation. In this section, we consider in more detail the properties of approximations based on PSWFs. We first show that for the single wave $\cos(M\pi x)$, with the optimal $c = M\pi$, the continuous PSWF expansion converges exponentially fast when at least two PSWFs are retained per wavelength. Equivalently, two points per wavelength are required for exponential convergence of the discrete approximation. This should be contrasted with about π points per wavelength needed for methods using classical orthogonal polynomials.

The second result pertains to the approximation of a general smooth function with a finite series of PSWFs. Recall that, for an unknown function, the optimal choice of the bandwidth parameter, c, is unknown and the approximation depends on two parameters, c and N. A natural approach is assume that the parameters are related and our experiments show that $c = N$ is a good choice if we want to maintain the full accuracy (16 digits). We explain why we cannot use $c \geq (\pi/2)N$ and illustrate that there can be benefits in taking $c \simeq (\pi/2)N$, albeit at the price of a lower accuracy.

3.1. Approximation of waves-points per wavelength. Let us consider the wave $u(x) = e^{iM\pi x}$. It follows directly from (2.1) and Theorem 2.1 that its PSWF expansion is

$$e^{iM\pi x} = \sum_{j=0}^{+\infty} \left(\lambda_j \psi_j^c(1)\right) \psi_j^c(x), \tag{3.1}$$

where $c = M\pi$.

Note that

$$|\lambda_j \psi_j^c(1)|^2 = |\lambda_j||\lambda_j \psi_j^c(1)^2|,$$

where the term $\lambda_j \psi_j^c(1)^2$ is the jth term in the expansion of $e^{i\pi M}$ (cf. (3.1)) and thus bounded—in fact it tends to zero with growing j. From [19], we know that $|\lambda_j|$ decays exponentially with j if $j > \frac{2c}{\pi} = 2M$. This establishes the result: *The accurate resolution of a wave requires two PSWFs per wave.* We recall here that expansions based on Chebyshev or Legendre polynomials require about π points per wave. Only mapped methods [20] may achieve similar resolution results for sufficiently high values of N.

In Figure 3.1, we plot the L^2-error of the truncated PSWF expansion of the function $\cos(M\pi x)$ versus $\frac{N}{M}$ (N is the number of terms in the expansion). It clearly confirms that when $N/M > 2$ the error decays exponentially.

In the above discussion we took $c = M\pi$, which is optimal. However, for general functions, we do not have a simple optimal c (see Figure 3.2) where we display the interpolation results with the PSWFs for two different functions. Clearly, the optimal c depends on the required accuracy and the function being approximated. This is due to the fact that an arbitrary function has many different modes and each mode has a distinct optimal c.

Downloaded 11/26/12 to 128.148.252.35. Redistribution subject to SIAM license or copyright; see http://www.siam.org/journals/ojsa.php

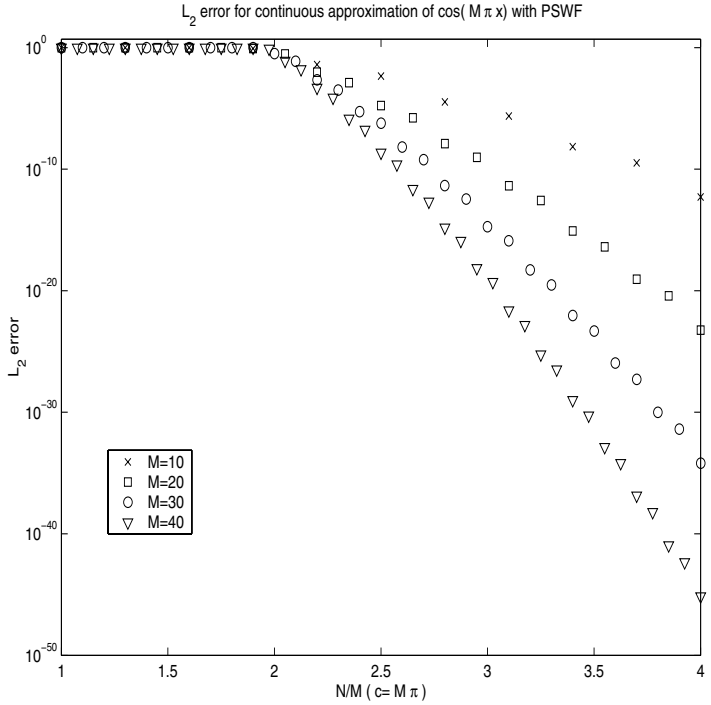

FIG. 3.1. *L^2-error of the PSWF expansion (truncated after N terms) of $\cos(M\pi x)$ versus N/M. $\times$: $M = 10$; $\square$: $M = 20$; $\circ$: $M = 30$; $\bigtriangledown$: $M = 40$.*

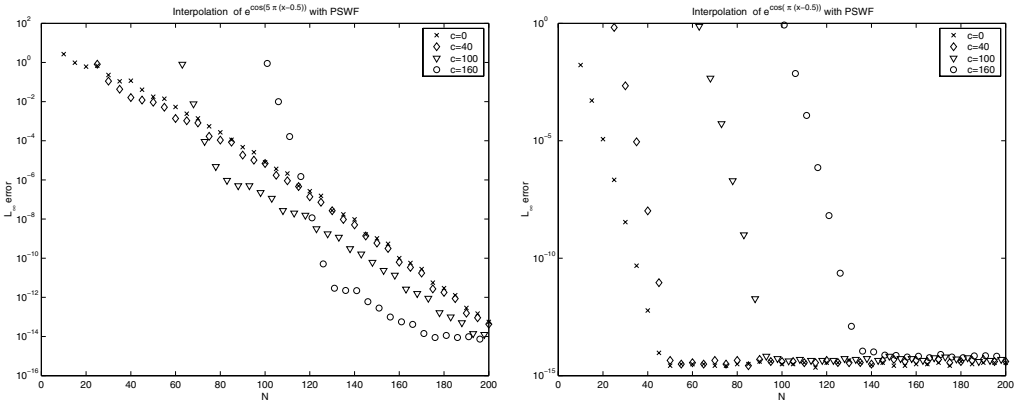

FIG. 3.2. *Demonstration that the optimal c, if it exists, depends on the specific problem and the required accuracy. Left: L_∞-error for the interpolation of $e^{\cos(5\pi(x-0.5))}$. For an error around 10^{-6}, $c = 100$ is the best choice. For an error as small as 10^{-10}, $c = 160$ is optimal. Right: L_∞-error for the interpolation of $e^{\cos(\pi(x-0.5))}$. Clearly, $c = 0$ (Legendre basis) is the best among the four choices.*

3.2. Error estimates. In this section, we consider the error estimates, in a Sobolev norm, of the PSWF expansion of a smooth function. Let $x \in [-1, 1]$, and consider the expansion $u(x) = \sum_{k=0}^{+\infty} \hat{u}_k \psi_k^c(x)$. The order of the convergence of the

Downloaded 11/26/12 to 128.148.252.35. Redistribution subject to SIAM license or copyright; see http://www.siam.org/journals/ojsa.php

partial sum $u_N(x) = \sum_{k=0}^{N} \hat{u}_k \psi_k^c(x)$ is determined by

$$\|u - u_N\|^2_{L^2[-1,1]} \leq \sum_{k=N+1}^{\infty} |\hat{u}_k|^2,$$

i.e., it depends solely on the decay rate of the coefficients $\{\hat{u}_k\}$.

Using the standard notation of $H^s[-1,1]$ for the Sobolev space of functions with distributional derivatives up to order s being square integrable in $L^2[-1,1]$, we prove in the appendix the following theorem.

THEOREM 3.1. *Assume that $u \in H^s[-1,1]$ with the PSWF expansion $u(x) = \sum_{i=0}^{+\infty} \hat{u}_i \psi_i^c(x)$.*

If $q_N = \sqrt{\frac{c^2}{\chi_N}} < 1$, then

$$|\hat{u}_N| \leq D\left(N^{-\frac{2}{3}s}\|u\|_{H^s[-1,1]} + (q_N)^{\delta N}\ \|u\|_{L^2[-1,1]}\right), \tag{3.2}$$

where both δ and D are positive constants.

From (3.2) it is evident that the expansion coefficients, $\hat{u}_N$, may exhibit spectral convergence when $q_N < 1$. In [23], it is shown that if n grows with c as

$$n = \frac{2}{\pi}\left[c + b\,\log(2\sqrt{c})\right]$$

for some b, then

$$\chi_n \sim c^2 + 2bc + O(1).$$

Thus

$$q_n < 1 \Leftrightarrow \chi_n > c^2 \Leftrightarrow b > 0 \Leftrightarrow n > \frac{2}{\pi}c.$$

Consequently, the finite PSWF expansion of a smooth function, $u \in C^\infty[-1,1]$,

$$\sum_{k=0}^{N} \hat{u}_k \psi_k^c(x)$$

is spectrally accurate if and only if

$$N > \frac{2}{\pi}c.$$

In Figure 3.3, we display the relationship between N and c ensuring that $q_N \leq 1$, obtained directly by solving the eigenvalue problem. This clearly confirms the above result. Figure 3.4 shows the loss of accuracy as N approaches $\frac{2}{\pi}c$. The loss of accuracy partially confirms Theorem 3.1. More precisely, the second term in (3.2) is dominant as N approaches $\frac{2}{\pi}c$, i.e., q_N approaches one. When q_N is very close to one, $(q_N)^{\delta N}$ cannot be small for any moderate N.

We notice that $c = N$ (which guarantees that q_N is bounded away from one) appears to be a good choice if one requires maximum accuracy, although larger values of c may also work if a reduced accuracy is acceptable. In section 4, we will further discuss the issue of choosing c when also considering the time-step and discrete stability.

Similar results are obtained when we use the PSWFs to interpolate a smooth function. In Figure 3.5, we compare interpolations based on PSWF and Chebyshev polynomials. Here we choose the number of grid points $N = c$. The results indicate that the PSWF interpolation is superior for functions with fine structures.

Downloaded 11/26/12 to 128.148.252.35. Redistribution subject to SIAM license or copyright; see http://www.siam.org/journals/ojsa.php

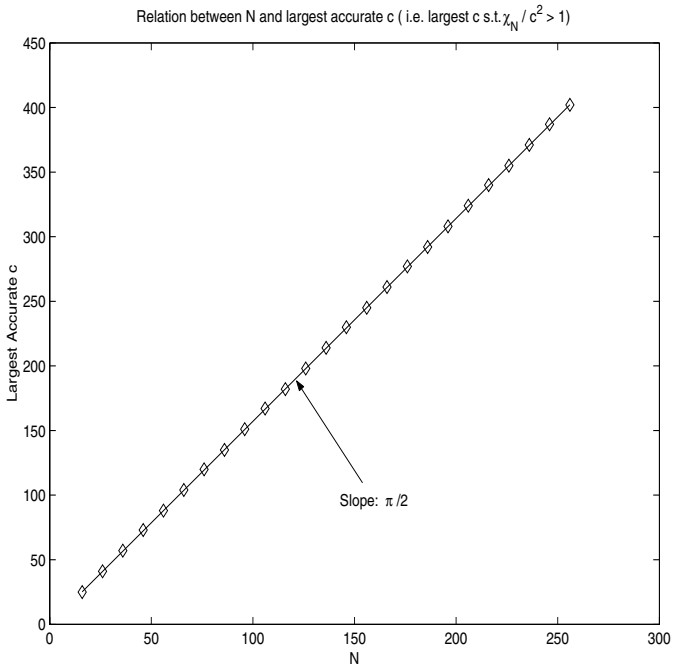

FIG. 3.3. *Computational validation of the relation between N and the biggest c which makes $q_N \leq 1$. The slope is $\pi/2$, as predicted in the text.*

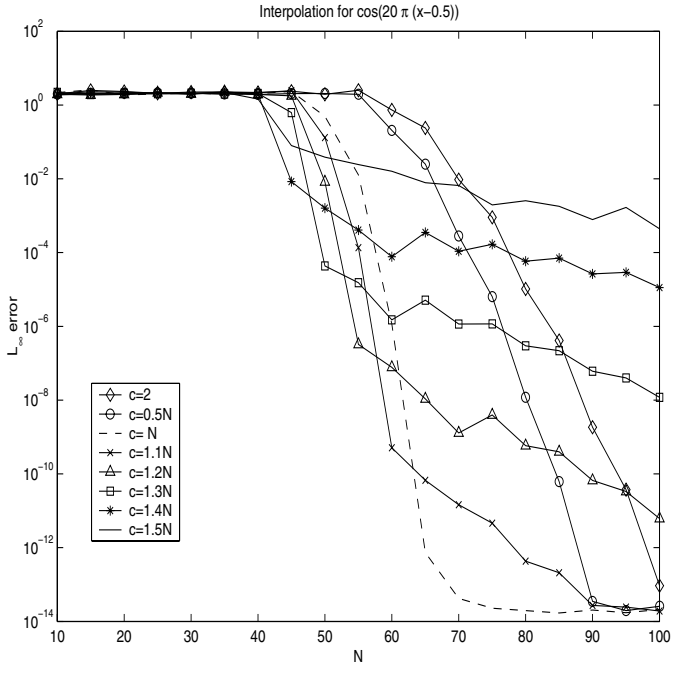

FIG. 3.4. *The loss of accuracy as c approaches $\frac{\pi}{2}N$.*

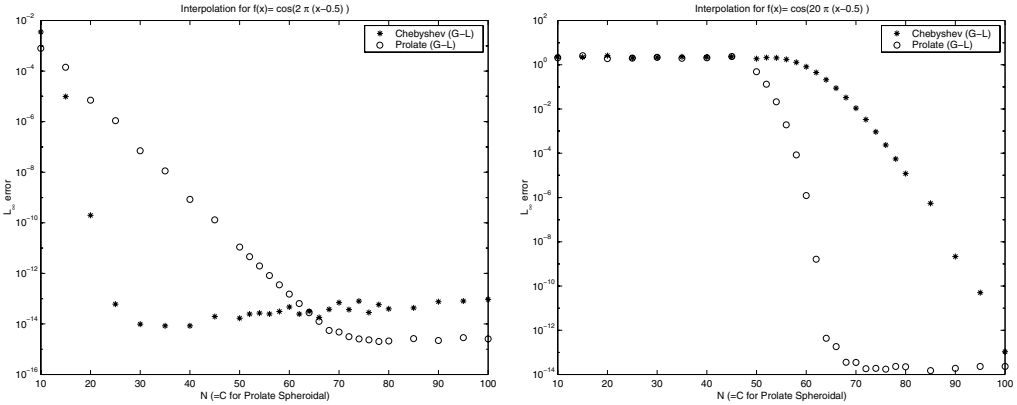

FIG. 3.5. *Interpolation results.* ○: *Prolate spheroidal wave basis;* ∗: *Chebyshev polynomials basis.* $c = N$ *for prolate spheroidal wave basis. Left:* $f(x) = \cos(2\pi(x - 0.5))$. *Right:* $f(x) = \cos(20\pi(x - 0.5))$.

4. Solving PDEs. In the following we shall discuss the use of the PSWFs as a basis in spectral methods for solving wave problems. Particular attention shall be paid to issues of semidiscrete and fully discrete stability.

4.1. First order wave equation. Consider the first order one-way wave equation

$$\begin{cases} u_t = u_x, & x \in [-1, 1], \\ u(1, t) = g(t), \\ u(x, 0) = f(x) \end{cases} \tag{4.1}$$

for which we shall seek a numerical solution.

Consider the interpolation points $\{x_0, \ldots, x_N\}$ which will be specified later. We define the Prolate–Lagrange function as $L_j(x) = \sum_{k=0}^{N} l_{jk}\psi_k^c(x)$ such that $L_j(x_k) = \delta_{jk}$. The existence of Prolate–Lagrange functions follows from the fact that the PSWFs form a Chebyshev system [17].

In a penalty Galerkin approximation we seek an approximation to the wave problem of the form

$$u_N(x, t) = \sum_{j=0}^{N} u_N(x_j, t)L_j(x)$$

such that the vector $\vec{U} = (u_N(x_0, t), \ldots, u_N(x_N, t))^T$ satisfies the equation

$$M\frac{d\vec{U}}{dt} = S\vec{U} - \tau(u_N(1, t) - g(t))\vec{e}_N. \tag{4.2}$$

Here, the boundary condition is imposed in a penalty way [7, 12, 15]. The matrices $M = (m_{jk})$ and $S = (s_{jk})$ are defined as

$$m_{jk} = \int_{-1}^{1} L_j(x)L_k(x)\,dx, \tag{4.3}$$

$$s_{jk} = \int_{-1}^{1} L_j(x)L_k'(x)\,dx, \tag{4.4}$$

Downloaded 11/26/12 to 128.148.252.35. Redistribution subject to SIAM license or copyright; see http://www.siam.org/journals/ojsa.php

Downloaded 11/26/12 to 128.148.252.35. Redistribution subject to SIAM license or copyright; see http://www.siam.org/journals/ojsa.php

and $\vec{e}_N = (0, \ldots, 1)^T$.

THEOREM 4.1 (stability). *The semidiscrete method described in* (4.2) *is stable for* $\tau \geq 1/2$.

Proof. For the stability proof it suffices to assume that $g(t) = 0$. Multiplying (4.2) by $\vec{U}^T$, we get

$$\begin{aligned}\frac{1}{2}\frac{d}{dt}\left(\vec{U}^T M \vec{U}\right) &= \sum_{jk} u_N(x_j,t) s_{kj} u_N(x_k,t) - \tau u_N(1,t)^2 \\ &= \sum_{jk} \int_{-1}^{1} u_N(x_j,t) u_N(x_k,t) L_j(x) L_k'(x)\, dx - \tau u_N(1,t)^2 \\ &= \int_{-1}^{1} u_N(x,t) \frac{\partial u_N(x,t)}{\partial x} - \tau u_N(1,t)^2 \\ &= \frac{1}{2}\left(u_N(1,t)^2 - u_N(-1,t)^2 - 2\tau u_N(1,t)^2\right).\end{aligned}$$

Thus, if $\tau \geq \frac{1}{2}$, then

$$\frac{d}{dt} \sum_{jk} \int_{-1}^{1} u_N(x_j,t) u_N(x_k,t) L_j(x) L_k(x)\, dx \leq 0$$

or

$$\frac{d}{dt} \int_{-1}^{1} \left(u_N(x,t)\right)^2\, dx \leq 0.$$

This proves the theorem. ∎

One way to implement the pseudospectral (collocation) method is to replace the integrals in (4.3) and (4.4) by quadrature formulas based on the points $\{x_k\}$. Alternatively, one can substitute the approximation $u_N(x,t)$ for u into the PDE (4.1) and require that the obtained equation is satisfied at certain collocation points (in most cases $\{x_k\}$ are used as collocation points as well).

For the PSWF collocation method, we do not have a stability proof. The difficulty is caused by the fact that the product of any two of the first N PSWFs with band-limit c is not in the space spanned by the first $2N$ PSWFs with band-limit $2c$ for which the PSWF quadrature is exact. However, when using $\{x_k\}$ as the collocation points, we numerically verify that the eigenvalues of the differentiation matrix have negative real parts.

We shall consider two sets of grid points as $\{x_k\}$: the Gauss–Lobatto PSWF points (one way to compute them is given in [8]) and the zeros of $(1-x^2)(\psi_N^{2c})'$. Note that these points must be computed from PSWF with band-limit $2c$ (see [25]). As we find the performance of the methods based on these two sets of points to be almost equivalent, the latter will be used for the PSWF collocation method if not specified otherwise.

When using explicit time discretization, e.g., Runge–Kutta schemes, one faces a stability limit on the time-step Δt. A necessary condition for stability is that the product of Δt and the largest eigenvalue of the differential matrix, being $M^{-1}(S - \tau \vec{e}_N \vec{e}_N^T)$ in the current scheme, is inside the stability region of the time-stepping scheme.

In Figure 4.1, we observe that for fixed N the magnitude of the largest eigenvalue λ of the PSWF collocation method decreases when c/N increases. So without violating

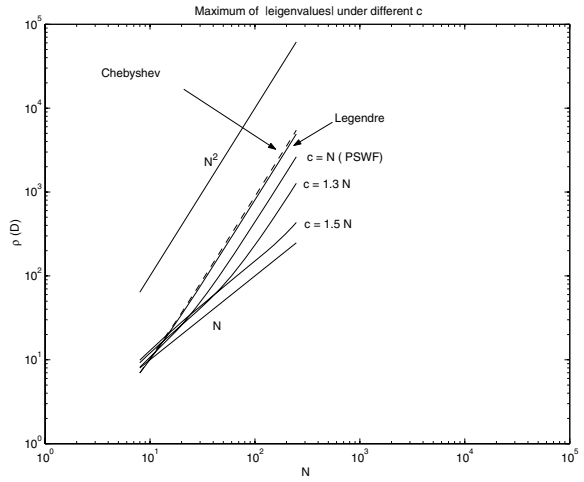

FIG. 4.1. *The largest absolute eigenvalue of the PSWF collocation method using different values of c, and the Chebyshev and Legendre collocation methods.*

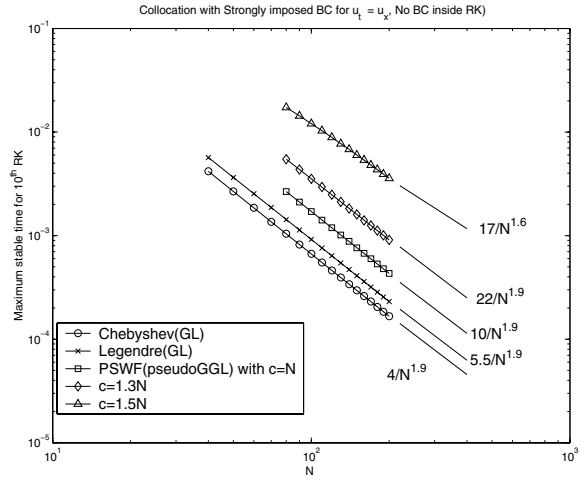

FIG. 4.2. *The largest stable time-step for the PSWF collocation method using different values of c, the Chebyshev and Legendre collocation methods. A* 10*th order explicit Runge–Kutta scheme was used.*

the stability condition, a larger c leads to larger Δt, as confirmed by Figure 4.2. When computing the largest stable time-step, we implemented a 10th order explicit Runge–Kutta scheme, the general form (mth order) for $u_t = Au$ with constant matrix A being given as [6]

$$\begin{aligned} u_1 &= u^n + \frac{\Delta t}{m}\, Au^n, \\ u_k &= u^n + \frac{\Delta t}{m+1-k}\, Au_{k-1}, \qquad k = 2, \ldots, m-1, \\ u^{n+1} &= u^n + \Delta t\, Au_{m-1}. \end{aligned}$$

Downloaded 11/26/12 to 128.148.252.35. Redistribution subject to SIAM license or copyright; see http://www.siam.org/journals/ojsa.php

Downloaded 11/26/12 to 128.148.252.35. Redistribution subject to SIAM license or copyright; see http://www.siam.org/journals/ojsa.php

This ensures that the errors from the time integration are negligible.

In Figure 4.2, the largest stable time-step approaches a growth rate $O(N^{-\frac{3}{2}})$, when c goes to $(\pi/2)N$. This suggests that one can use a time-step of order $O(N^{-\frac{3}{2}})$ by letting $c = (\pi/2)N$. However, this choice of c causes a loss of accuracy, as demonstrated in Figure 3.4. In Table 4.1, we list the errors for the time-steps shown in Figure 4.2. It is evident that the accuracy is decreasing when c approaches $(\pi/2)N$. This is consistent with our analysis for the approximation using PSWFs.

TABLE 4.1

L_∞-error when solving $u_t = u_x$ for $u(x,t) = \cos(2\pi(x+t-0.5))$ with collocation methods. A 10th order explicit Runge–Kutta is used. For each N of each method, Δt is the largest stable time-step shown in Figure 4.2.

N	80	120	160	200
Chebyshev	3.453×10^{-14}	4.952×10^{-14}	1.521×10^{-13}	1.115×10^{-13}
Legendre	7.361×10^{-14}	1.117×10^{-12}	1.274×10^{-12}	1.592×10^{-12}
PSWF($c = N$)	9.770×10^{-15}	9.104×10^{-15}	2.081×10^{-14}	1.482×10^{-14}
PSWF($c = 1.3N$)	3.638×10^{-1}	2.860×10^{-9}	7.133×10^{-12}	9.137×10^{-14}
PSWF($c = 1.5N$)	5.022×10^{-2}	2.968×10^{-1}	8.051×10^{-2}	1.649×10^{-4}

The PSWF method offers a systematic way of balancing accuracy and stability. As a compromise, $c = N$ is used in all subsequent numerical tests. This yields a time-step which is twice the one obtained by a Legendre collocation method without sacrificing accuracy. Similar results can be obtained by using a mapping technique [16]. In some cases it may be beneficial to use a different value of c, e.g., in Figure 3.4, $c = 1.1N$ could be used if only about 10^{-9} accuracy was required. Similar improvements over the traditional Chebyshev collocation methods can also be achieved by the mapping technique which was first presented in [18], albeit at a loss of the quadrature. However, it will be impractical to use the PSWF collocation method if one wants to change c very often, as both the interpolation points and the differentiation matrix have to be recomputed when c is changed.

4.1.1. Numerical tests. The following numerical tests were carried out with a collocation method that determines a nodal approximation $u_N(x,t) = \sum_{j=0}^{N} u_N(x_j,t)L_j(x)$ such that the equation

$$\frac{\partial u_N}{\partial t} - \frac{\partial u_N}{\partial x} = 0 \tag{4.5}$$

is satisfied at the grid points $\{x_j\}$. The boundary condition is applied either strongly or by a penalty procedure as discussed above.

We considered three different initial conditions, listed in Table 4.2.

TABLE 4.2

Initial condition $f(x)$.

Smooth	Nonsmooth
$\cos(2\pi(x-0.5))$	
$\cos(20\pi(x-0.5))$	$\sin(20\pi(x-0.5)) + H(x-0.5)$

The Heaviside function $H(x)$ is defined as

$$H(x) = \begin{cases} 1 & \text{if } x \le 0, \\ -1 & \text{otherwise.} \end{cases} \tag{4.6}$$

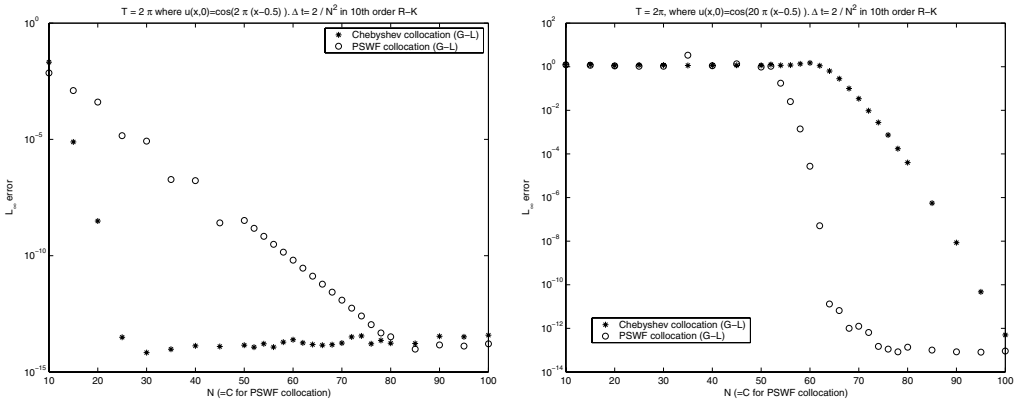

FIG. 4.3. *L_∞-error from solving $u_t = u_x$ with a collocation method and strongly imposed boundary condition. Final time: $T = 2\pi$. 10th order Runge–Kutta with $\Delta t = \frac{2}{N^2}$. Left: $u(x,t) = \cos(2\pi(x - 0.5 + t))$. Right: $u(x,t) = \cos(20\pi(x - 0.5 + t))$. ○: PSWF; ∗: Chebyshev.*

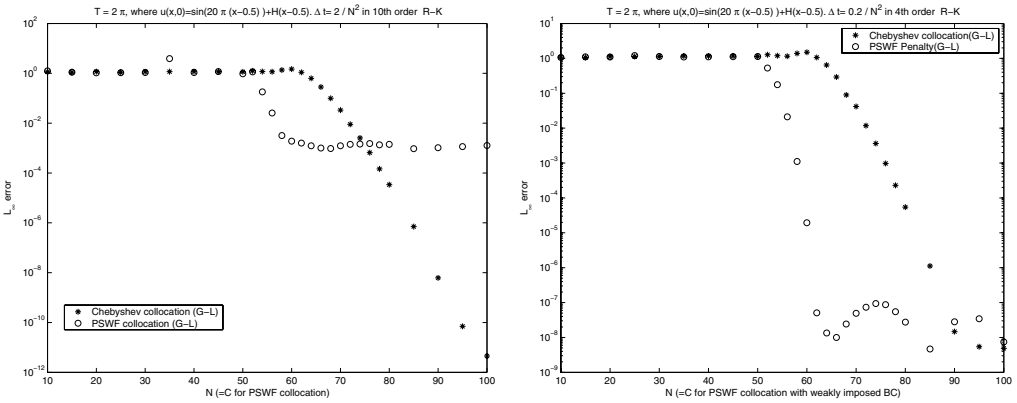

FIG. 4.4. *L_∞-error of solving $u_t = u_x$ by collocation methods. $u(x,0) = \sin(20\pi(x - 0.5)) + H(x - 0.5)$. Final time: $T = 2\pi$. Left: Chebyshev and PSWF collocation methods with strongly imposed boundary condition. Right: PSWF collocation method with weakly imposed boundary condition.*

In Figure 4.3, we show the errors from solving (4.5) with these smooth initial conditions. The Chebyshev method performs better for functions with small wave numbers, whereas the PSWF method is clearly better for functions with large wave numbers.

In Figure 4.4, we present the errors for the discontinuous initial condition. In this case the solution is discontinuous and the point of discontinuity propagates towards the boundary with a speed $a = 1$. We observe that the error does not decay below 10^{-4} when using a strongly imposed boundary condition.

When the boundary condition is imposed by a penalty procedure [7, 15, 12], the PSWF method is superior to the Chebyshev method (see the right part of Figure 4.4). We also applied the Legendre collocation method to solve the equation with discontinuous initial conditions. Similar to the PSWF collocation method, the weakly imposed boundary condition yields more accurate results than the strongly imposed boundary condition.

The improved performance with the weak imposition of the boundary condition

Downloaded 11/26/12 to 128.148.252.35. Redistribution subject to SIAM license or copyright; see http://www.siam.org/journals/ojsa.php

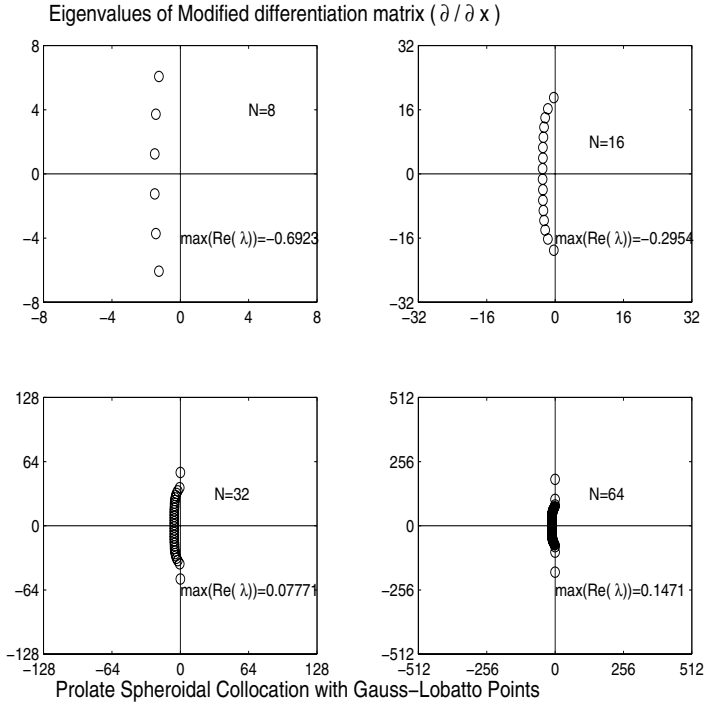

FIG. 4.5. *Eigenvalues of the differentiation matrix for the PSWF collocation method. Boundary condition is imposed strongly.*

can be linked to the behavior of the differentiation matrix. Figures 4.5 and 4.6 show the spectrum of the modified differentiation matrix for the PSWF collocation method with strongly and weakly imposed boundary conditions, respectively. We believe that the positive real parts of eigenvalues for $N = 32$ and 64 in Figure 4.5 are spurious and caused by round-off errors, as discussed in [24] for Chebyshev/Legendre spectral differentiation matrices. These results document the importance of imposing boundary conditions in a penalty way.

4.2. A cavity problem. In this section, we solve the one-dimensional Maxwell equations

$$\begin{cases} \epsilon \dfrac{\partial E}{\partial t} = \dfrac{\partial H}{\partial x}, \\ \mu \dfrac{\partial H}{\partial t} = \dfrac{\partial E}{\partial x}, \end{cases} \tag{4.7}$$

where $E(x,t)$ and $H(x,t)$ are the tangential electric and magnetic fields, and ϵ and μ are the relative permittivity and permeability of the materials.

We shall consider the test case of a one-dimensional cavity $[-1,1]$ filled with two dielectric media with a material interface at $x = 0$. Two perfectly conducting walls are located at $x = -1$ and $x = 1$. Denote by ϵ_1 and μ_1 the relative permittivity and permeability of the material at $[-1,0]$. Similarly, ϵ_2 and μ_2 are the relative permittivity and permeability of the material in $[0,1]$. The electric and magnetic fields in the two domains are denoted by E_1, H_1 and E_2, H_2.

Downloaded 11/26/12 to 128.148.252.35. Redistribution subject to SIAM license or copyright; see http://www.siam.org/journals/ojsa.php

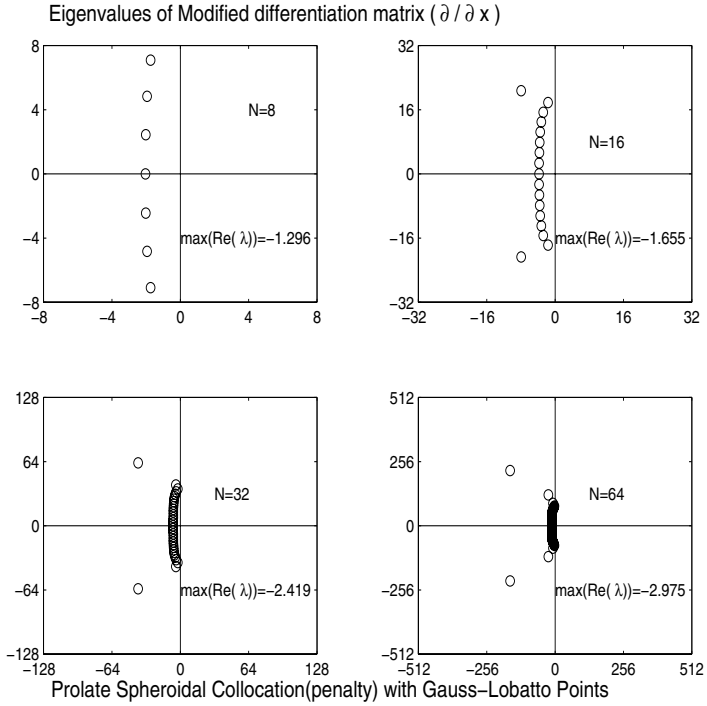

FIG. 4.6. *Eigenvalues of the differentiation matrix for the PSWF collocation method. Boundary condition is imposed weakly.*

Since the walls are perfectly conducting, the boundary conditions are

$$E_1(-1,t) = 0 \quad \text{or} \quad \frac{\partial H_1}{\partial x}|_{x=-1} = 0,$$

$$E_2(1,t) = 0 \quad \text{or} \quad \frac{\partial H_2}{\partial x}|_{x=1} = 0.$$

Denote $n_1 = \sqrt{\epsilon_1}$ and $n_2 = \sqrt{\epsilon_2}$, i.e., $\{n_i\}$ is the index of refraction. In all the following tests, we assume $\mu_1 = \mu_2 = 1.0$, $n_1 = 1$, and $n_2 = 10$.

In Figure 4.7, we display the solution at $t = 0$. (See [9] for the derivation of the exact solution.) When $n_1 \neq n_2$, the solution loses smoothness at the material interface. It is only globally C^0 in $[-1, 1]$. Thus without using domain decomposition, we can only get second order convergence with a Chebyshev or PSWF collocation method (see Figure 4.8). Because of this low order there is limited advantage to the use of the PSWF collocation method, although the PSWF method needs fewer points per wavelength to resolve the solution.

For the pointwise errors from both PSWF and Chebyshev collocations, there is a spike (Figure 4.9) propagating into the left-half domain and whose speed is the speed of a characteristic wave. It is caused by the initial condition being computed from the exact solution to the PDE, rather than an exact solution to the numerical scheme. One can remedy this by computing the initial conditions from the numerical scheme.

Downloaded 11/26/12 to 128.148.252.35. Redistribution subject to SIAM license or copyright; see http://www.siam.org/journals/ojsa.php

Downloaded 11/26/12 to 128.148.252.35. Redistribution subject to SIAM license or copyright; see http://www.siam.org/journals/ojsa.php

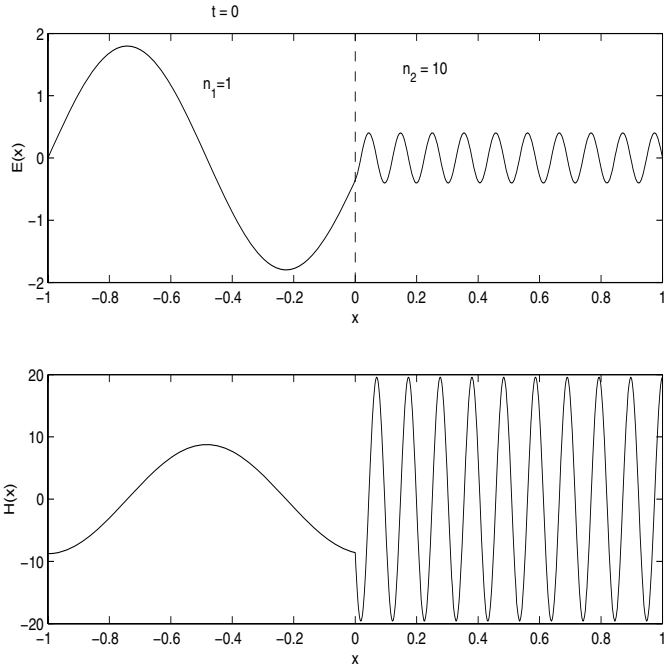

FIG. 4.7. *Exact solution at $t = 0$, $n_1 = 1.0$, $n_2 = 10.0$. Upper: electric field $E(x,t)$. Lower: magnetic field $H(x,t)$.*

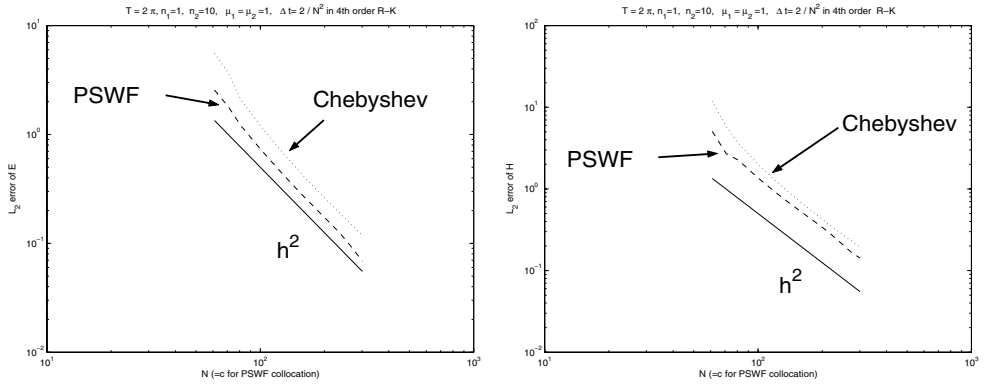

FIG. 4.8. *The discrete L_2-error at $t = 2\pi$. Strongly imposed boundary condition for the Chebyshev collocation method, weakly imposed boundary condition for the PSWF collocation method. Left: electric field $E(x,t)$. Right: magnetic field $H(x,t)$.*

Assume that the semidiscrete equation of (4.7) is

$$\begin{cases} \dfrac{d\vec{E}}{dt} = D_H\ \vec{H}, \\ \dfrac{d\vec{H}}{dt} = D_E\ \vec{E}. \end{cases} \tag{4.8}$$

Downloaded 11/26/12 to 128.148.252.35. Redistribution subject to SIAM license or copyright; see http://www.siam.org/journals/ojsa.php

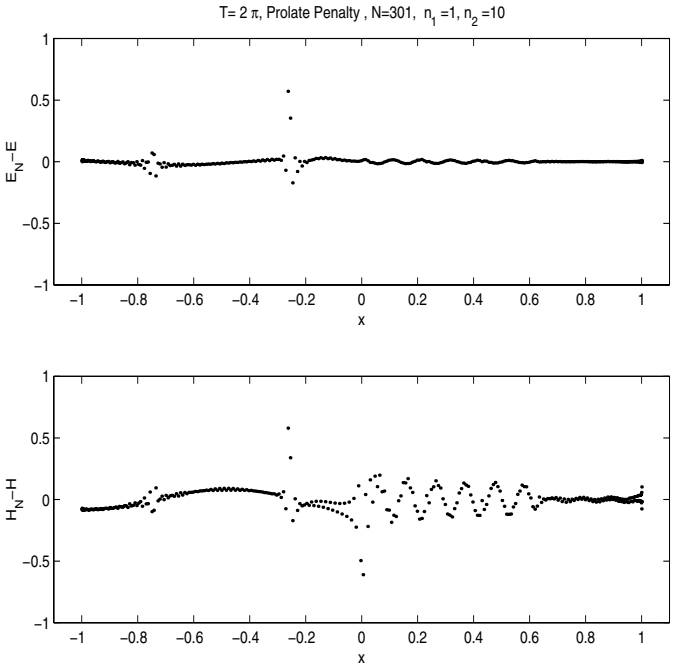

FIG. 4.9. *Pointwise error from the PSWF collocation method.* $c = N = 301$. $t = 2\pi$. *Upper: electric field. Lower: magnetic field.*

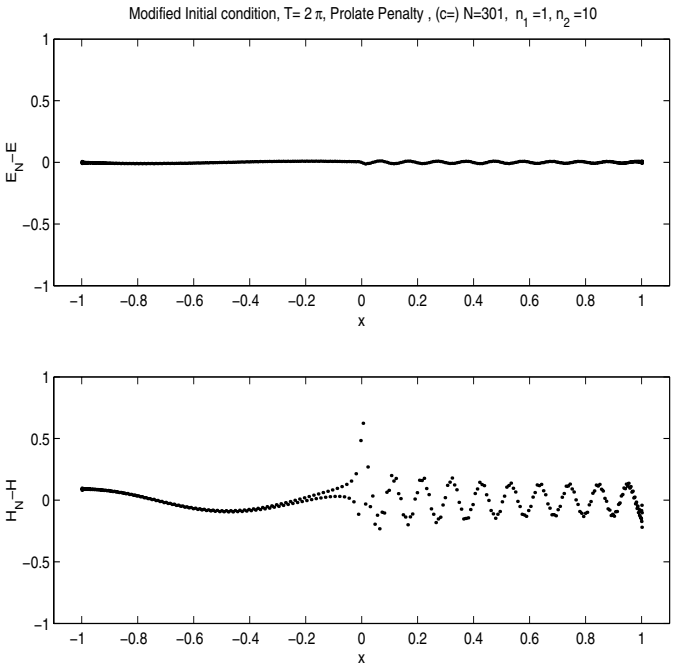

FIG. 4.10. *Pointwise errors with the initial conditions computed from the numerical scheme.*

Downloaded 11/26/12 to 128.148.252.35. Redistribution subject to SIAM license or copyright; see http://www.siam.org/journals/ojsa.php

Take the exact solution to the numerical scheme as $\vec{E} = \tilde{\vec{E}} e^{i\omega t}$ and $\vec{H} = \tilde{\vec{H}} e^{i\omega t}$, and introduce them into (4.8) to obtain an eigenvalue problem,

$$i\omega \begin{pmatrix} \tilde{\vec{E}} \\ \tilde{\vec{H}} \end{pmatrix} = \begin{pmatrix} 0 & D_H \\ D_E & 0 \end{pmatrix} \begin{pmatrix} \tilde{\vec{E}} \\ \tilde{\vec{H}} \end{pmatrix}.$$

The eigenvectors can be used as the initial conditions for the numerical scheme. The new results are shown in Figure 4.10, confirming this to be the source of the spike.

5. Conclusions. Our study of the applicability of PSWF-based methods to the numerical solution of time-dependent PDEs results in the following conclusions:

- The PSWF approximation requires two points per wavelength to resolve a single mode wave function ($\cos(m\pi x)$) if c is chosen as $c = m\pi$.
- Approximating a broadband function $u(x)$ by a finite expansion of the form $\sum_{n=0}^{N} \hat{u}_n \psi_n^c$, one obtains spectral accuracy for $N > \frac{2}{\pi} c$ with loss of accuracy when N approaches the limit. A robust choice is $N = c$.
- When solving the wave equation $u_t = u_x$ with explicit temporal schemes, the CFL bound on the time-step increases as $c \leq (\pi/2)N$ increases. Asymptotically, $\Delta t = O(N^{-3/2})$ if c is very close to $(\pi/2)N$. However, this choice results in a deterioration of the accuracy. We found $c = N$ to be a good choice to ensure good accuracy and large stable time-step, the latter effectively increasing by a factor of 2 over methods based on classical orthogonal polynomials.
- For marginally resolved broadband problems, the PSWF-based method with a carefully chosen c is better than the Legendre/Chebyshev collocation methods. Fewer points are needed per wavelength for fast convergence and the allowable time-step is twice as large.
- The weak imposition of the boundary condition is necessary for the success of the method for problems with discontinuous initial conditions. By weakly applying the boundary condition, we improve the spectrum of the first order differentiation matrix of the PSWF collocation method, i.e., moving those eigenvalues with almost zero real parts a little distance away from the imaginary axis, thus introducing a small amount of dissipation.

Appendix. In this appendix, we prove Theorem 3.1.

Let $\beta_k = \beta_k^N$ be the coefficient in the expansion of ψ_N^c in terms of the normalized Legendre polynomials, i.e., $\psi_N^c(x) = \sum_{k=0}^{+\infty} \beta_k^N \overline{P}_k(x)$, where

$$\beta_k = \int_{-1}^{1} \overline{P}_k(x) \psi_N(x)\, dx.$$

The following recurrence relation for β_k is proven in [25]:

$$\begin{aligned} \frac{(k+2)(k+1)}{(2k+3)\sqrt{(2k+5)(2k+1)}}\, \beta_{k+2} = &\left(\frac{\Lambda - k(k+1)}{c^2} - \frac{2k(k+1)-1}{(2k+3)(2k-1)} \right) \beta_k \\ &- \frac{k(k-1)}{(2k-1)\sqrt{(2k-3)(2k+1)}}\, \beta_{k-2}. \end{aligned} \tag{A.1}$$

Note that, from [23], $\Lambda = \chi_N = O(N^2)$. Let m be any integer satisfying

$$m = O(\Lambda^{1/3}) = O(N^{2/3}) \quad \text{and} \quad 2m(2m+1) < \frac{\ln 2}{2} \Lambda. \tag{A.2}$$

Downloaded 11/26/12 to 128.148.252.35. Redistribution subject to SIAM license or copyright; see http://www.siam.org/journals/ojsa.php

Then we have the following lemma.

LEMMA A.1. *Assume* $q = q_N = \sqrt{\frac{c^2}{\Lambda}} < 1$. *Then for any given* $k \le 2m$, β_k *is bounded by*

$$|\beta_k| \le \begin{cases} D\left(\frac{2}{q}\right)^k |\beta_0|, & k \text{ even}, \\ D\left(\frac{2}{q}\right)^k |\beta_1|, & k \text{ odd}, \end{cases} \tag{A.3}$$

where D *is a constant independent of* m.

Proof. We give the proof only for even k. The proof for odd k is similar.

Rewrite (A.1) as

$$\beta_{k+2} = \frac{1}{f(k+2)} \left(\frac{1}{q^2} \left(1 - \frac{k(k+1)}{\Lambda} \right) - g(k) \right) \beta_k - \frac{f(k)}{f(k+2)} \beta_{k-2}, \tag{A.4}$$

where $f(x) = \frac{x(x-1)}{(2x-1)\sqrt{(2x-3)(2x+1)}}$ and $g(x) = \frac{2x(x+1)-1}{(2x+3)(2x-1)}$. It is easy to verify that

$$1/4 \le f(x) \le 2\sqrt{5}/15, \qquad \frac{1}{2} \le g(x) \le \frac{11}{21} \qquad \text{for } x \ge 2.$$

Therefore, $f(x)/f(x+2) \le 8\sqrt{5}/15$ when $x \ge 2$.

Since

$$k \le 2m \Rightarrow \frac{1}{q^2} \left(1 - \frac{k(k+1)}{\Lambda} \right) \ge \frac{1}{q^2} \left(1 - \frac{\ln 2}{2} \right) > \frac{11}{21} \ge g(x) \qquad \text{for } x \ge 2,$$

the coefficient of β_k in (A.4) is positive. Hence, if we assume (A.3) is true for $k, k-2$, we can bound β_{k+2} as

$$\begin{aligned} |\beta_{k+2}| &\le \frac{1}{f(k+2)} \left(\frac{1}{q^2} \left(1 - \frac{k(k+1)}{\Lambda} \right) - g(k) \right) |\beta_k| + \frac{f(k)}{f(k+2)} |\beta_{k-2}| \\ &\le 4 \frac{1}{q^2} \left(1 - \frac{\ln 2}{2} \right) D \left(\frac{2}{q} \right)^k |\beta_0| + \frac{8\sqrt{5}}{15} D \left(\frac{2}{q} \right)^{k-2} |\beta_0| \\ &\le D \left(\frac{2}{q} \right)^{k+2} \left(1 - \frac{\ln 2}{2} + \frac{\sqrt{5} q^4}{30} \right) |\beta_0| \le D \left(\frac{2}{q} \right)^{k+2} |\beta_0|. \end{aligned}$$

The last inequality follows from the facts that $q < 1$ and $1 - \frac{\ln 2}{2} + \frac{\sqrt{5}q^4}{30} < 1$. When $k = 0, 2$, (A.3) can be easily satisfied by modifying the constant D. This completes the proof. ∎

Define

$$A_k = \int_{-1}^{1} x^k \psi_N^c(x)\, dx. \tag{A.5}$$

One can check that $\sqrt{2}\beta_0 = A_0$ and $\sqrt{2/3}\beta_1 = A_1$.

LEMMA A.2. *Let* m *be an integer satisfying* (A.2). *Then*

$$|A_0| \le K q^{2m} \sqrt{\frac{2}{4m+1}}, \tag{A.6}$$

Downloaded 11/26/12 to 128.148.252.35. Redistribution subject to SIAM license or copyright; see http://www.siam.org/journals/ojsa.php

where K is a constant independent of m.

Proof. We first show that

$$|A_0| \le q^{2m}|A_{2m}| \prod_{l=1}^{m-1} \frac{1}{1-\frac{2l(2l+1)}{\Lambda}}. \tag{A.7}$$

Rewrite (2.2) as

$$\left((1-x^2)\psi'\right)' + \Lambda(1-q^2x^2)\psi = 0.$$

For $l \le m$, multiply the above equation by x^{2l}, then integrate on $[-1,1]$ to obtain

$$\begin{cases} 2l(2l-1)A_{2l-2} + (\Lambda - 2l(2l+1))\,A_{2l} - \Lambda q^2 A_{2l+2} = 0, & l \ge 1, \\ A_0 - q^2 A_2 = 0, & l = 0. \end{cases}$$

Since $2m(2m+1) \le \Lambda$, all $A_0, A_2, \ldots, A_{2m+2}$ have the same sign. Thus

$$|A_{2l}| \le q^2\,|A_{2l+2}|\frac{\Lambda}{\Lambda - 2l(2l+1)} \le q^2\,|A_{2l+2}|\frac{1}{1-\frac{2l(2l+1)}{\Lambda}}.$$

Then (A.7) follows by induction.

To show (A.6), we note that $1 - x \ge e^{-2x}$ when $0 \le x \le \frac{\ln 2}{2}$. Therefore,

$$1 - \frac{2l(2l+1)}{\Lambda} \ge e^{-2\frac{2l(2l+1)}{\Lambda}} \qquad \text{if } l = 1, 2, \ldots, m-1,$$

which leads to

$$\prod_{l=1}^{m-1} \frac{1}{1-\frac{2l(2l+1)}{\Lambda}} \le e^{\frac{\sum_{l=1}^{m-1} 4l(2l+1)}{\Lambda}} \le e^{\frac{\frac{8}{3}m^3}{\Lambda}}.$$

From (A.2), $m = O(\Lambda^{1/3})$. So (A.5) yields

$$|A_{2m}| \le \|x^{2m}\|_{L^2[-1,1]}\,\|\psi\|_{L^2[-1,1]} \le \sqrt{\frac{2}{4m+1}},$$

which proves (A.6). ∎

In the same way, one can also show that $|A_1| \le Kq^{2m}\sqrt{\frac{2}{4m+3}}$ under the same conditions on m. We are now ready to prove Theorem 3.1.

Proof of Theorem 3.1. Assume $u(x)$ has the Legendre expansion

$$u(x) = \sum_{k=0}^{+\infty} a_k P_k(x).$$

By definition,

$$\hat{u}_N = \int_{-1}^{1} u(x)\psi_N(x)\,dx = \int_{-1}^{1} \psi_N(x)\left(\sum_{k=0}^{+\infty} a_k P_k(x)\right)dx.$$

Let M be an integer such that

$$\frac{M+1}{2m} = \gamma\frac{\ln(1/q)}{\ln(2/q)}, \tag{A.8}$$

Downloaded 11/26/12 to 128.148.252.35. Redistribution subject to SIAM license or copyright; see http://www.siam.org/journals/ojsa.php

where m is defined in (A.2) and $0 < \gamma < 1$ is a constant. Denote by $u_M(x)$ the partial sum $u_M(x) = \sum_{k=0}^{M} a_k P_k(x)$. Then

$$\hat{u}_N = \int_{-1}^{1} u_M(x)\psi_N(x)\,dx \;+\; \int_{-1}^{1} (u(x) - u_M(x))\,\psi_N(x)\,dx.$$

We use I and II to represent the first and second terms, respectively. According to the error estimate of the Legendre approximation [11, 6],

$$|II| \le \|u - u_M\|_{L^2[-1,1]}\, \|\psi_N(x)\|_{L^2[-1,1]} \le DM^{-s}\|u\|_{H^s[-1,1]},$$

where D is a constant (in the following, D is used for different constants). Now,

$$\begin{aligned}
|I| &= \left|\sum_{k=0}^{M} a_k \int_{-1}^{1} P_k(x)\psi_N(x)\,dx\right| = \left|\sum_{k=0}^{M}\left(a_k\sqrt{\frac{2}{2k+1}}\right)\;\left(\int_{-1}^{1}\overline{P}_k(x)\psi_N(x)\,dx\right)\right| \\
&\le \left(\sum_{k=0}^{M}(a_k)^2\frac{2}{2k+1}\right)^{1/2}\;\left(\sum_{k=0}^{M}\left(\int_{-1}^{1}\overline{P}_k(x)\psi_N(x)\,dx\right)^2\right)^{1/2} \\
&\le \|u\|_{L^2[-1,1]}\;\left(\sum_{k=0}^{M}\beta_k^2\right)^{1/2} \\
&\le D\|u\|_{L^2[-1,1]}\;\left(\sum_{k=0}^{M}\left(\frac{2}{q}\right)^{2k}\right)^{1/2}\;\max\,(|\beta_0|,|\beta_1|).
\end{aligned}$$

Here Lemma A.1 is used in the last reduction.

From Lemma A.2, $\beta_0 = \frac{1}{\sqrt{2}}A_0 < Kq^{2m}\sqrt{\frac{2}{4m+1}}$ and $\beta_1 = \sqrt{3/2}A_1 < Kq^{2m}\sqrt{\frac{2}{4m+3}}$, where K is a constant. Thus

$$\begin{aligned}
|I| &\le D\|u\|_{L^2[-1,1]}\;\left(\sum_{k=0}^{M}\left(\frac{2}{q}\right)^{2k}\right)^{1/2}\;q^{2m}\sqrt{\frac{2}{4m+3}} \\
&\le D\|u\|_{L^2[-1,1]}\;\left(\frac{2}{q}\right)^{M+1}\;q^{2m}\sqrt{\frac{2}{4m+3}} \\
&\le D\|u\|_{L^2[-1,1]}\;\left(q\left(\frac{2}{q}\right)^{\frac{M+1}{2m}}\right)^{2m}\sqrt{\frac{2}{4m+3}} \\
&\le D\|u\|_{L^2[-1,1]}\,p^{2m}\sqrt{\frac{2}{4m+3}},
\end{aligned}$$

where $p = q(\frac{2}{q})^{\frac{M+1}{2m}}$.

From (A.8), $p = q^{1-\gamma}$ and $M = O(m) = O(N^{2/3})$. Combining the bounds for I and II, we get

$$|\hat{u}_N| \le D\left(N^{-\frac{2}{3}s}\|u\|_{H^s[-1,1]} + (q_N)^{\frac{2}{3}(1-\gamma)N}\;\|u\|_{L^2[-1,1]}\right),$$

which proves Theorem 3.1 with $\delta = \frac{2}{3}(1-\gamma)$. ∎

Acknowledgments. We thank John Boyd for sharing his work [5] before publication. We would also like to thank the anonymous referees who helped improve the manuscript markedly.

Downloaded 11/26/12 to 128.148.252.35. Redistribution subject to SIAM license or copyright; see http://www.siam.org/journals/ojsa.php

REFERENCES

[1] R. Baltensperger and J.-P. Berrut, *The linear rational collocation method,* J. Comput. Appl. Math., 134 (2001), pp. 243–258.
[2] A. Bayliss and E. Turkel, *Mappings and accuracy for Chebyshev pseudo-spectral approximations,* J. Comput. Phys., 101 (1992), pp. 349–359.
[3] G. Beylkin and K. Sandberg, *Wave propagation using bases for bandlimited functions,* Wave Motion, 41 (2005), pp. 263–291.
[4] J. P. Boyd, *Approximation of an analytic function on a finite real interval by a bandlimited function and conjectures on properties of prolate spheroidal functions,* Appl. Comput. Harmon. Anal., 15 (2003), pp. 168–176.
[5] J. P. Boyd, *Prolate spheroidal wave functions as an alternative to Chebyshev and Legendre polynomials for spectral element and pseudospectral algorithms,* J. Comput. Phys., 199 (2004), pp. 688–716.
[6] C. Canuto, M. Y. Hussaini, A. Quarteroni, and T. A. Zang, *Spectral Methods in Fluid Dynamics,* Springer-Verlag, Berlin, 1988.
[7] M. H. Carpenter and D. Gottlieb, *Spectral methods on arbitrary grids,* J. Comput. Phys., 129 (1996), pp. 74–86.
[8] H. Cheng, V. Rokhlin, and N. Yarvin, *Nonlinear optimization, quadrature, and interpolation,* SIAM J. Optim., 9 (1999), pp. 901–923.
[9] A. Ditkowski, K. Dridi, and J. S. Hesthaven, *Convergent Cartesian grid methods for Maxwell's equations in complex geometries,* J. Comput. Phys., 170 (2001), pp. 39–80.
[10] W. S. Don and A. Solomonoff, *Accuracy enhancement for higher derivative using Chebyshev collocation and a mapping technique,* SIAM J. Sci. Comput., 18 (1997), pp. 1040–1055.
[11] D. Funaro, *Polynomial Approximation of Differential Equations,* Lecture Notes in Phys. 8, Springer-Verlag, Berlin, 1992.
[12] D. Funaro and D. Gottlieb, *A new method of imposing boundary conditions in pseudospectral approximations of hyperbolic equations,* Math. Comp., 51 (1988), pp. 599–613.
[13] D. Gottlieb, M. Y. Hussaini, and S. A. Orszag, *Theory and application of spectral methods,* in Spectral Methods for Partial Differential Equations, R. Voigt, D. Gottlieb, and M. Y. Hussaini, eds., SIAM, Philadelphia, PA, 1984, pp. 1–54.
[14] D. Gottlieb and S. A. Orszag, *Numerical Analysis of Spectral Methods: Theory and Applications,* CBMS-NSF Regional Conf. Ser. in Appl. Math., SIAM, Philadelphia, 1977.
[15] J. S. Hesthaven, *Spectral penalty methods,* Appl. Numer. Math., 33 (2000), pp. 23–41.
[16] J. S. Hesthaven, P. G. Dinsen, and J. P. Lynov, *Spectral collocation time-domain modeling of diffractive optical elements,* J. Comput. Phys., 155 (1999), pp. 287–306.
[17] S. Karlin and W. Studden, *Tchebysheff Systems with Applications in Analysis and Statistics,* Interscience, New York, 1966.
[18] D. Kosloff and H. Tal-Ezer, *A modified Chebyshev pseudospectral method with an $O(N^{-1})$ time step restriction,* J. Comput. Phys., 104 (1993), pp. 457–469.
[19] H. J. Landau and H. Widom, *Eigenvalue distribution of time and frequency limiting,* J. Math. Anal. Appl., 77 (1980), pp. 468–491.
[20] J. L. Mead and R. A. Renaut, *Accuracy, resolution, and stability properties of a modified Chebyshev method,* SIAM J. Sci. Comput., 24 (2002), pp. 143–160.
[21] S. C. Reddy, J. A. C. Weideman, and G. F. Norris, *On a Modified Chebyshev Pseudospectral Method,* Report, Oregon State University, 1999.
[22] D. Slepian and H. O. Pollak, *Prolate spheroidal wave functions, Fourier analysis, and uncertainty.* I, Bell Syst. Tech. J., 40 (1961), pp. 43–64.
[23] D. Slepian, *Prolate spheroidal wave functions, Fourier analysis, and uncertainty.* IV: *Extensions to many dimensions, generalized prolate spheroidal wave functions,* Bell Syst. Tech. J., 43 (1964), pp. 3009–3058.
[24] L. N. Trefethen and M. R. Trummer, *An instability phenomenon in spectral methods,* SIAM J. Numer. Anal., 24 (1987), pp. 1008–1023.
[25] H. Xiao, V. Rokhlin, and N. Yarvin, *Prolate spheroidal wave functions, quadrature and interpolation,* Inverse Problems, 17 (2001), pp. 805–838.